

Some topics at the interface of strongly nonlinear space and fusion plasma physics

R. O. Dendy

Citation: *AIP Conf. Proc.* **1320**, 23 (2011); doi: 10.1063/1.3544331

View online: <http://dx.doi.org/10.1063/1.3544331>

View Table of Contents: <http://proceedings.aip.org/dbt/dbt.jsp?KEY=APCPCS&Volume=1320&Issue=1>

Published by the [American Institute of Physics](#).

Related Articles

Topology of tokamak plasma equilibria with toroidal current reversal

Phys. Plasmas **19**, 012504 (2012)

The dynamics of ion with electrostatic waves in a sheared magnetic field

Phys. Plasmas **18**, 122104 (2011)

Fluid and drift-kinetic description of a magnetized plasma with low collisionality and slow dynamics orderings. II. Ion theory

Phys. Plasmas **18**, 102506 (2011)

Self-similar nonlinear dynamical solutions for one-component nonneutral plasma in a time-dependent linear focusing field

Phys. Plasmas **18**, 084502 (2011)

Tokamak equilibria with non field-aligned axisymmetric divergence-free rotational flows

Phys. Plasmas **18**, 072502 (2011)

Additional information on AIP Conf. Proc.

Journal Homepage: <http://proceedings.aip.org/>

Journal Information: http://proceedings.aip.org/about/about_the_proceedings

Top downloads: http://proceedings.aip.org/dbt/most_downloaded.jsp?KEY=APCPCS

Information for Authors: http://proceedings.aip.org/authors/information_for_authors

ADVERTISEMENT



AIP Advances

Submit Now

Explore AIP's new
open-access journal

- Article-level metrics now available
- Join the conversation! Rate & comment on articles

Some topics at the interface of strongly nonlinear space and fusion plasma physics

R O Dendy^{1,2}

¹Euratom/UKAEA Fusion Association, Culham Science Centre, Abingdon, Oxfordshire, OX14 3DB, U.K.

²Centre for Fusion, Space and Astrophysics, Department of Physics, Warwick University, Coventry, CV4 7AL, U.K.

1. Introduction

The overall phenomenology of plasmas emerges from multiple couplings between processes on many different lengthscales and timescales, creating innumerable feedback loops. For example, overall energy confinement – the central emergent property for fusion – is governed by a self-consistent loop involving: temperature, density, and current profiles extending from the extremely hot core to the cold edge; collective instabilities which are locally triggered when profile gradients exceed certain limits, and which draw their free energy from the profiles; the saturated turbulence which is driven by these instabilities; and the energy transport resulting from this turbulence, which in turn reacts back on the temperature and current profiles. This nonlinear feedback loop is built up from plasma processes which, individually, are nonlinear. Plasmas typically coexist with magnetic fields, whose energy density is often comparable to the thermal or bulk flow kinetic energies of the plasma. It follows that magnetic fields affect the system's behaviour on all lengthscales and timescales from those of electron gyromotion to those characteristic of the entire system – these differ by factors of 10^4 for length and 10^{10} for time in fusion experiments, for example. Fusion plasma confinement properties thus emerge from self organisation within a complex system[1-3]; this fact was early recognised[4], but not always pursued energetically thereafter; for a recent review, see Ref.[5]. The need to quantify, interpret, predict, and control this emergent phenomenology is central to the mission of plasma physicists, whether for fusion or in the geospace environment.

2. Two brief remarks on nonlinear plasma physics and complex systems science

First, complex systems science seeks to identify simple universal models[1,6] that capture the key physics of extended macroscopic systems, whose behaviour is governed by multiple nonlinear coupled processes that operate across a wide range of spatiotemporal scales. In such systems, energy release often occurs intermittently, in bursty events, and the phenomenology can exhibit scaling, that is, a significant degree of self-similarity. Within plasma physics, such systems include Earth's magnetosphere, the solar corona, and toroidal magnetic confinement experiments. Guided by broad understanding of the dominant plasma processes – for example, turbulent transport in tokamaks, or magnetic reconnection in some space and solar contexts – we construct minimalist complex systems models that yield relevant global behaviour. Examples include the sandpile approach to tokamaks[7-12] and to the magnetosphere[13-20], and the reconnecting[21] multiple-loops model[22] for the solar coronal magnetic carpet[23]. Such

models can address questions that are inaccessible to analytical treatment and are too demanding for computational resolution. These models are useful, and potentially valid, if they can replicate aspects of observed global phenomenology, or of event statistics, for which no explanation has been obtained from first principles including the underlying equations. For example, a simple sandpile model[10,24], which implements critical-gradient-triggered avalanching transport associated with nearest-neighbour mode coupling, generates[10,12] some of the distinctive observed elements of tokamak confinement phenomenology such as ELMing and edge pedestals. The same sandpile model also generates distributions of energy-release events whose statistics resemble those observed in the auroral zone[16]. Similarly, a simple multiple-loops model[22], which implements random photospheric footpoint motion combined with reconnection of intersecting oriented loops, generates global magnetic field structure resembling the solar coronal magnetic carpet, with power law distributions for energy-release events that are similar to those observed in the solar corona[25-28].

Finding complex systems models whose behaviour resembles that of large-scale plasmas helps to identify the dominant physical processes that govern the observed phenomenology. Such models may enable one to isolate a small set of control parameters – perhaps representing the combined effects of several observational experimental variables – whose values determine system behaviour. A simple model that captures the key physics can provide a means to both understand and control the overall system behaviour.

The second remark is that complex systems science offers an array of statistical physics techniques that are specially adapted to capturing and quantifying the nonlinear features of macroscopic system behaviour. As noted by Kadomtsev[7] in 1992, for example, diffusive and Gaussian paradigms for the transport arising from turbulence in tokamak plasmas cannot account for all the confinement phenomenology observed, furthermore bursty transport is widely seen. The review paper Ref.[29] describes how several techniques of time series analysis were successfully applied to measurements and observations of strongly nonlinear phenomena in a variety of plasmas including astrophysical accretion discs[30,31], the solar corona[32], edge fluctuations in the MAST tokamak[33], ELM statistics in the JET tokamak[34], and the solar wind and terrestrial ionosphere[35,36]. Progress continues with further applications to the MAST tokamak[37], LHD stellarator[38], and solar wind[39-41], some of which we review here.

3. Capturing strong nonlinearity in fusion plasmas by means of statistical physics techniques

The extent to which universal properties are displayed by edge plasma turbulence in toroidal magnetically confined plasmas is an important but unresolved question. Particularly interesting is the identification of generic features that may be shared by edge plasma turbulence in the three most promising confinement concepts: conventional tokamaks, spherical tokamaks, and stellarators. Any generic feature would arise in all three confinement systems, and would display universal characteristics; for example, their statistical properties, when rescaled with respect to the size of the device and other key bulk parameters, would be the same. Their identification thus requires quantitative comparison of the measured turbulence properties under different operating regimes for the different confinement systems, which in turn requires the application of modern techniques for the statistical analysis of nonlinear time series. As an example, we consider recent

analyses[33,37,38] of probe measurements of the ion saturation current I_{sat} obtained from the plasma edge in the world-leading spherical tokamak MAST[33,37] and in the world's leading stellarator, the Large Helical Device[38]. In the latter case we address datasets previously described in Ref.[42].

We first examine scaling properties of the absolute moments $S_m = \langle |\delta x(t, \tau)|^m \rangle \propto \tau^{\zeta(m)}$ of fluctuations $\delta x(t, \tau) = \sum_{t'=t}^{t+\tau-1} I_{sat}(t')$ with varying temporal scale τ , and obtain scaling exponents $\zeta(m)$. The results shown in Fig.1, for example, demonstrate that the functional form of $\zeta(m)$, and

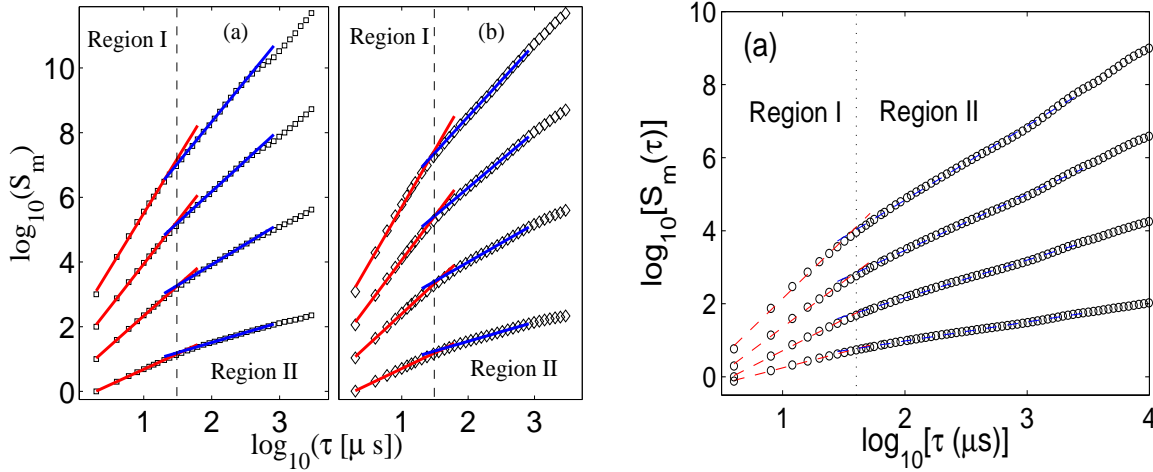


Fig.1 Logarithmic plots of structure functions S_m of order $m = 1$ to 4 versus temporal scale τ for edge turbulence measurement in: (Left) MAST from Ref.[37]; (Right) LHD from Ref.[38].

the values of scaling exponents are robust quantitative discriminators of the plasma turbulence. In addition to a well defined discontinuity at $40\mu s$, plots of $\log(S_m)$ versus $\log(\tau)$ demonstrate self-similar scaling $\zeta(m) = \alpha m$. The value of α is the same for all the MAST L-mode plasmas considered on timescales up to $40\mu s$, suggesting universality in the character of these fluctuations. On longer timescales $40\mu s$ to $400\mu s$, two distinct groups of scaling exponents are found, that exhibit weak dependence on magnetic field structure[37].

Significant quantitative results[37,38] also arise from investigations of the probability density functions (PDFs) of the I_{sat} fluctuations. These can be strongly non-Gaussian, in particular they are sometimes long-tailed through having significantly more large events. The PDF of the fluctuations from the MAST plasmas considered, sampled on a timescale $\tau = 2\mu s$, is well fitted by an extremal[3] Fréchet distribution with index $\alpha = 1.25$; see Fig.2(Left). For individual MAST plasmas, Fréchet distributions give the best fit for $\tau \leq 40\mu s$, and Gumbel for $\tau \geq 40\mu s$. This transition at $40\mu s$, which may correspond to filamentary structures observed in optical imaging, is confirmed by the structure function scaling properties $S_m \sim \tau^{\zeta(m)}$ noted in Fig.1(Left).

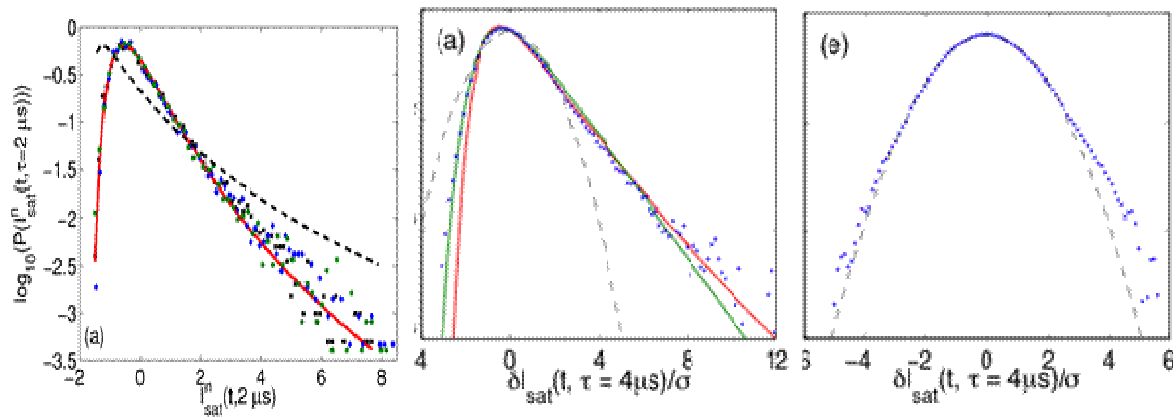


Fig.2 Probability density functions for turbulent edge plasma fluctuations. (Left): Sampled on two-microsecond timescales in the MAST edge plasma. (Centre): Sampled at a particular edge location in LHD on four-microsecond timescales. (Right): Sampled in LHD simultaneously with the central panel, at a location only a few millimetres away. Fitted curves relate to extreme value distributions, see Refs.[37,38] for details.

The left and centre panels of Fig.2 show that the short timescale fluctuations in MAST, and those at one location in LHD, are both well fitted by extreme value distributions, whereas a simple Gaussian provides a good fit to the LHD distribution at a second nearby location. This sheds light on shared, and different, physical behaviour at two levels. There is a broad question: to what extent are the measured statistical properties similar? And there is a more technical question: given that the stellarator edge magnetic structure encompasses both regular and stochastic field line regions, do these affect local turbulence measurements and do they relate to spherical tokamak scenarios where the edge magnetic field is deliberately stochasticised? Experiments involving the latter process are currently under way in MAST.

4. Capturing strong nonlinearity in astrophysical plasmas by means of statistical physics techniques

In a striking demonstration of their wide applicability, extreme event distributions[3] have been shown[30,31] to fit the PDFs of X-ray signal intensities emitted from the astrophysical accretion disc plasmas in the microquasar GRS 1915+105 and the black hole X-ray binary Cygnus X-1; see Fig.3. These accretion discs are formed by ambient plasma drawn towards, and orbiting around, stellar mass black holes, whose angular momentum prevents direct infall. Viscous outward transport of angular momentum within the disc enables matter at its inner edge to fall inwards, heating and radiating as it does so; the question whether accretion discs may be in a state of self organised criticality is discussed in Ref.[43]. As noted above[3], extreme value distributions result from repeatedly selecting the maximum value from each of a large number of

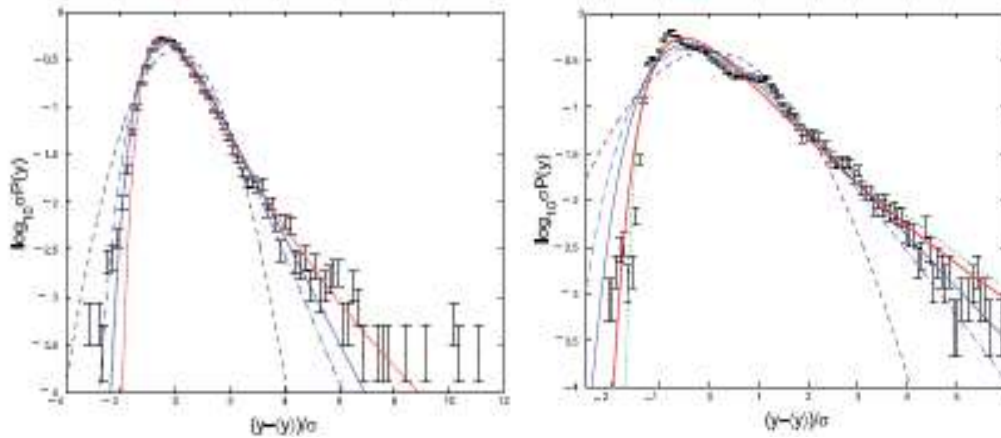


Fig.3 Long-tailed probability density functions of the X-ray signal intensity[30] observed from (Left) Cygnus X-1 and (Right) GRS 1915+105 accretion disc plasmas, showing strong deviation from the Gaussian (dashed black lines). The coloured curves represent best fits of different classes of known extreme value distribution functions to these long-tailed datasets.

large samples – the brightest among many contemporaneous local flashes scattered across an extended object, for example. The fact that the tails of the PDFs in Fig.3 can be fitted by extreme value distributions therefore suggests that the observed signals may be the brightest among multiple events occurring within each measurement window.

The observed signals are also found[30,31] to be self-similar. While self-similarity, like the non-Gaussian PDFs, is a strong indicator of highly-correlated processes such as turbulence, there are no *a priori* reasons to expect it in these contexts. Consider first the difference between the maximum and minimum values of a data time series $y(t)$ during an interval Δt ; this defines its range $R(\Delta t)$ for that interval. Run a window of width Δt through the entire dataset, yielding a value of $R(\Delta t)$ at each step. From these, an ensemble-averaged value $\langle R(\Delta t) \rangle$ is calculated, and this operation is then repeated for windows of different size Δt . If the time series $y(t)$ is self-similar, the ensemble-averaged value of the range scales with window size: $\langle R(\Delta t) \rangle = c\Delta t^H$, where c and H are constants. This equation defines the Hurst exponent H which quantifies the self-similar growth of range. Figure 4 displays the results of this procedure for the Cygnus X-1 and GRS 1915+105 datasets whose PDFs are shown in Fig.3, and for a set of edge turbulence measurements from the MAST tokamak. The well defined Hurst exponents demonstrate that the underlying nonlinear plasma physics gives rise to signals that are self-similar to a significant extent, implying turbulent processes with substantial correlation over long timescales – many days in the astrophysical cases. Furthermore, it is possible to quantify this self-similarity by means of the single model-independent quantity H . The value of H enables us to discriminate

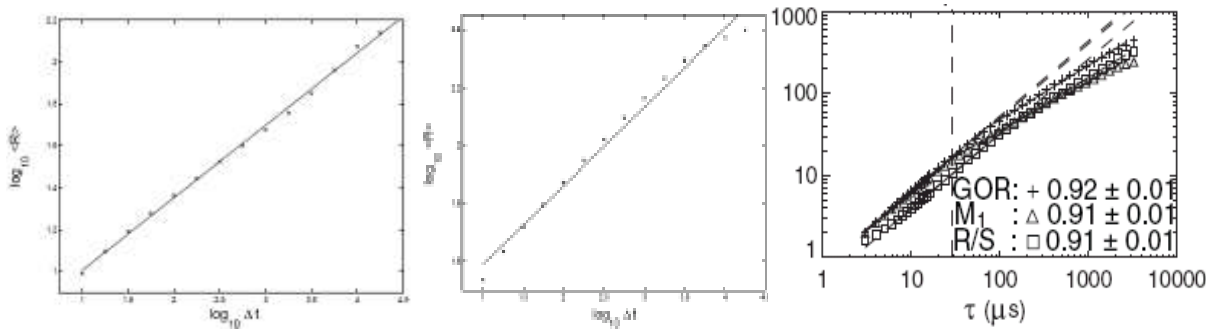


Fig.4 Growth of range. Logarithmic plots of $\langle R(\Delta t) \rangle$ versus Δt for: X-ray time series from Cygnus X-1(Left) and GRS 1915+105 (Centre)[30], where time steps are 90 minutes; and ion saturation current measurements in MAST L-mode plasma 6861 (Right)[33], where time units are microseconds, and several different algorithms for computing H are used. The value of the Hurst exponent is well defined in all cases: 0.35 ± 0.1 , 0.27 ± 0.2 , and 0.91 ± 0.01 , respectively.

observationally between datasets, and it constrains models of these systems. For example, a numerical simulation of MAST edge turbulence under the conditions of plasma 6861 should generate a signal whose H -value matches that obtained in Fig.4, and likewise for the astrophysical objects.

The differencing and rescaling technique[30] yields additional information on the timescales over which correlation persists in these instances of complex systems phenomenology within plasmas. The original data time series $y(t)$ is used to construct a differenced time series $Z(t, \tau) = y(t) - y(t - \tau)$. This time series gives the sequence of fluctuations in the data, over a timescale τ , at each time step. Many values of τ can be chosen, each of which generates a differenced time series $Z(t, \tau)$ describing fluctuations on the corresponding timescale. Thus a family of differenced time series $Z(t, \tau)$ is generated from a single data time series $y(t)$. Fluctuation amplitudes Z are typically small when τ is small, because the dataset does not have time to diverge, whereas larger-amplitude fluctuations Z occur for larger τ , during which interval the dataset has time to diverge substantially. In general, the distribution of fluctuations within the dataset on timescale τ is described by the probability density function $P(Z, \tau)$, known as the differenced distribution. For small τ , $P(Z, \tau)$ will typically be strongly peaked about $Z = 0$ and negligible for large Z , whereas $P(Z, \tau)$ will be significant at larger values of Z for larger τ .

If the fluctuations observed in the dataset are driven by a dominant underlying physical process which maintains correlation up to some timescale τ_c , and the fluctuations are self-similar, it follows that all members of the family of differenced distributions $P(Z, \tau: \tau < \tau_c)$ contain the same information. These distributions are, in essence, identical – they are simply stretched versions of each other. Figures 5 and 6 show this technique in action for Cygnus X-1 and MAST edge turbulence respectively. Figure 5 establishes that the X-ray output of Cygnus X-1 varies in a way

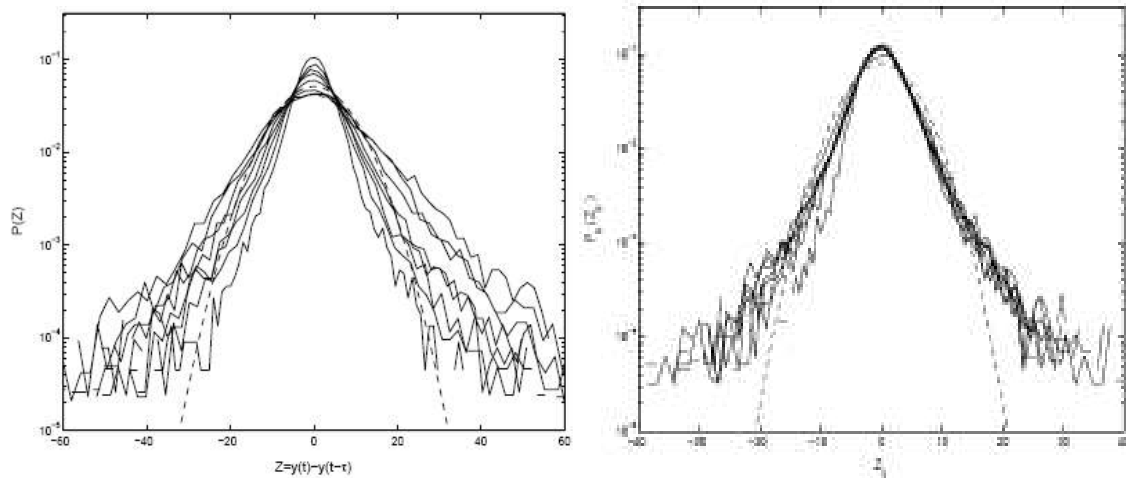


Fig.5 (Left) Unscaled PDFs $P(Z, \tau)$ of differenced time series of X-ray signals from Cygnus X-1, plotted versus Z , with differencing parameter τ stepping up in half-integer powers of the 90 minutes timestep up to a maximum 10^4 . Curves with lower $P(0)$ and broader tails correspond to higher values of τ . The scaling of $P(0)$ with τ yields the value of the parameter α used for rescaling. (Right) Rescaled PDFs $P_s(Z_s)$ plotted versus Z_s . The curves collapse onto a single characteristic distribution, which deviates substantially from a Gaussian (dashed line)[30].

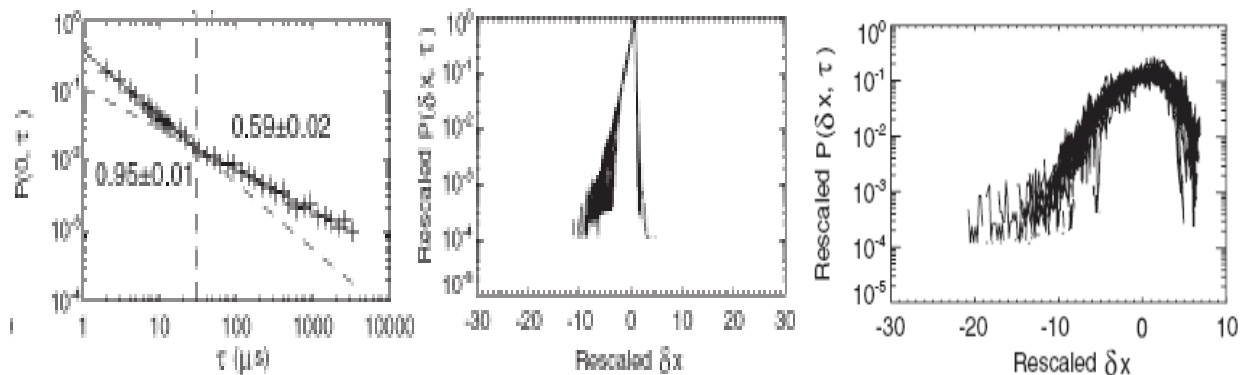


Fig.6 (Left) The value of $P(0, \tau)$ plotted versus τ for the family of differenced distributions $P(\delta x, \tau)$ constructed from ion saturation current (x) measurements in MAST L-mode plasma 6861. The scaling parameter α is well defined within two sharply separated regions. (Centre) Collapse of rescaled PDFs for $\tau < 60 \mu s$ onto a single curve, using slope 0.95 from left panel. (Right) Collapse of rescaled PDFs for $\tau > 60 \mu s$ onto a different single curve, using slope 0.59 from left panel[33].

which is self-similar and correlated. It is controlled by a single non-Gaussian process, on timescales up to three years[30]. For the data from GRS 1915+105, differencing and rescaling also operates successfully[30,31], but yields two well defined rescaling regimes with different values for the scaling parameter α , with correlations on timescales of days. This latter type of dual regime rescaling phenomenology is also found[33] for the MAST L-mode edge turbulence dataset analysed, with correlations on timescales of tens of microseconds; see Fig.6.

5. Capturing strong nonlinearity in solar wind plasmas by means of statistical physics techniques

The solar wind is a supersonic plasma flow which originates from the solar corona and propagates through interplanetary space, filling it until it reaches the local interstellar medium at the heliopause. It is evident from this description that the range of lengthscales and timescales on which solar wind physics unfolds is very extensive, furthermore solar wind fluctuations include both large scale episodic nonlinear perturbations and turbulence. The solar wind provides unique opportunities for long duration *in situ* studies of magnetohydrodynamic turbulence in a plasma flowing supersonically with high magnetic Reynolds number $\sim 10^5$. Its spectral power density scales approximately as inverse frequency f^{-1} at lower frequencies (≤ 1 mHz); and as $f^{-5/3}$ reminiscent of Kolmogorov's inertial range, at higher frequencies (~ 10 – 100 mHz). Both the $f^{-5/3}$ and f^{-1} fluctuations are often predominantly shear Alfvénic in character. The frequency at which the transition between power laws occurs (~ 1 – 10 mHz) is observed to decline with increasing heliocentric distance in the plane of the ecliptic, and this extension of the $f^{-5/3}$ range at greater distances can be interpreted as evidence for an evolving turbulent cascade. The f^{-1} range is taken to reflect embedded solar coronal turbulence, convected with the solar wind, while the large-scale magnetic structure of the corona varies with the solar cycle and heliospheric latitude, creating variations in solar wind speed.

The generic concept of extended self similarity (ESS) addresses[44] scaling in relevant non-ideal situations where, for example, the effects of dissipation on small scales or of finite system size on large scales inhibit the development of self similar behaviour over a wide range – for example, the formation of a broad inertial range of turbulence. Consider the structure function definition $S_m(\tau) = \langle y(t + \tau) - y(t) \rangle$, for which ideal scaling requires $S_m(\tau) \sim \tau^{\zeta(m)}$. ESS proceeds by replacing τ in the scaling expression by an initially unknown generalised timescale $g(\tau)$, such that $S_m(\tau) \sim [g(\tau)]^{\zeta(m)}$. It then follows that for structure functions of differing order p and q , $S_p(\tau) \sim [S_q(\tau)]^{\zeta(p)/\zeta(q)}$. Self similar behaviour is recaptured from the analysis of plots of $\log S_p(\tau)$ versus $\log S_q(\tau)$ for the datasets in question. Figure 7, from Ref.[40], shows this technique in action for the solar wind. The straight line fits imply a global scaling $\zeta(2)/\zeta(3) \sim 0.75$ with one per cent

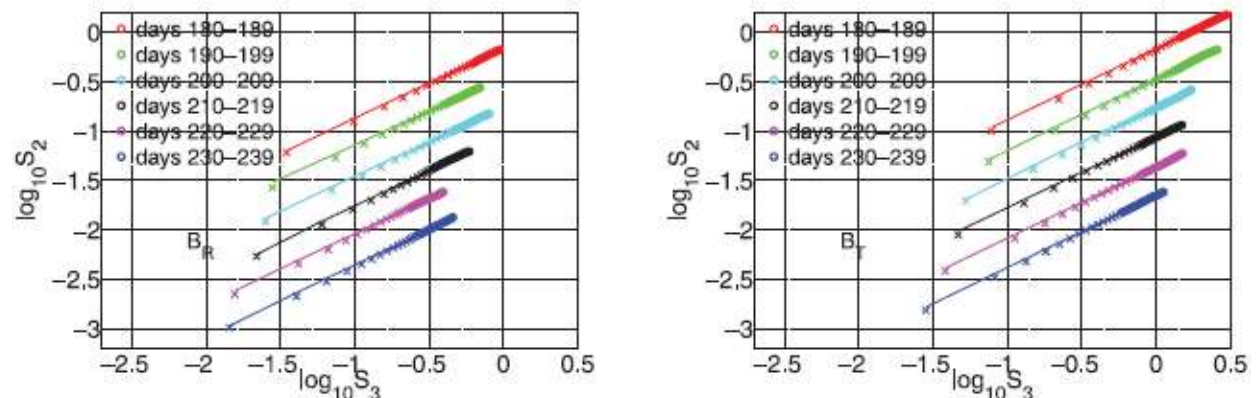


Fig.7 Evidence from Ref.[40] for extended self similarity in magnetic field fluctuations in the solar wind, showing (Left) radial component and (Right) tangential component. The measurements are grouped into contiguous 10-day periods, the plots for each of which are offset in the y-direction for clarity. The straight lines show linear regression fits across the full range of sampling intervals, from 2 to 49 minutes.

accuracy. Comparison of scaling between the $f^{-5/3}$ and f^{-1} ranges, and its dependence on heliocentric latitude and distance, are among the more technical ways of exploiting such results described in Ref.[40]. Here we simply note that a single robust quantitative measure of scaling has been extracted from the nonlinear complex system presented by the solar wind plasma.

6. Conclusions

In contrast to the situation twenty years ago, when plasma physics was wrestling alone with issues of strong nonlinearity and the global phenomenology that it generates, other branches of science are now engaged. The lateral flow of concepts and techniques at this frontier greatly assists progress.

Acknowledgments It is a pleasure to acknowledge the contributions of many collaborators to the application of complex systems science to plasma physics, including Sandra Chapman, Joe Dewhurst, Ben Dudson, Jon Graves, John Greenhough, Per Helander, Bogdan Hnat, Keith Hopcraft, David Hughes, Ken McClements, Thomas March, James Merrifield, Ruth Nicol, Maya Paczuski, George Rowlands, Nick Watkins and Robert Wicks. This work was supported in part by Euratom (but the views and opinions expressed herein do not necessarily reflect those of the European Commission) and by the United Kingdom Engineering and Physical Sciences Research Council. Figures from journal articles published previously are reproduced with kind permission of the respective publishers.

References

- [1] Bak P 1996 *How Nature Works* (New York: Copernicus)
- [2] Badii R and Politi A 1999 *Complexity* (Cambridge: Cambridge University Press)
- [3] Sornette D 2000 *Critical Phenomena in Natural Sciences* (Heidelberg: Springer)
- [4] Kadomtsev B B 1992 *Plasma Phys. Control. Fusion* **34** 1931
- [5] Dendy R O, Chapman S C and Paczuski M 2007 *Plasma Phys. Control. Fusion* **49** A95
- [6] Bak P, Tang C and K Wiesenfeld K 1987 *Phys. Rev. Lett.* **59**, 381
- [7] Newman D E, Carreras B A, Diamond P H and Hahm T S 1996 *Phys. Plasmas* **3**, 1858
- [8] Dendy R O and Helander P 1997 *Plasma Phys. Control. Fusion* **39**, 1947
- [9] Sanchez R, Newman D E and Carreras B A 2001 *Nucl. Fusion* **41** 247
- [10] Chapman S C, Dendy R O and Hnat B 2001 *Phys. Rev. Lett.* **86**, 2814
- [11] Graves J P, Dendy R O, Hopcraft K I and Jakeman E 2002 *Phys Plasmas* **9**, 1596
- [12] Chapman S C, Dendy R O and Hnat B 2003 *Plasma Phys. Control. Fusion* **45** 301
- [13] Consolini G 1997 *Cosmic Physics in the Year 2000* (Bologna, Italy: Società Italiana di Fisica) p 123
- [14] Chapman S C, Watkins N W, Dendy R O, Helander P and Rowlands G 1998 *Geophys. Res. Lett.* **25** 2397
- [15] Watkins N W, Chapman S C, Dendy R O, Helander P and Rowlands G 1999 *Geophys. Res. Lett.* **26** 2617
- [16] Lui A T Y, Chapman S C, Liou K, Newell P T, Meng C I, Brittnacher and Parks G K 2000 *Geophys. Res. Lett.* **27** 911

- [17] Watkins N W, Freeman M P, Chapman, S C and Dendy R O 2001 *J. Atmos. Solar-Terr. Phys.* **63** 1435
- [18] Chapman S C, Dendy R O and Hnat B 2001 *Phys. Plasmas* **8** 1969
- [19] Hnat B, Chapman S C, Rowlands G, Watkins N W and Freeman M P 2003 *Geophys. Res. Lett.* doi 10.1029/2003GL018209
- [20] Chapman S C, Dendy R O and Watkins N W 2004 *Plasma Phys. Control. Fusion* **46** B157
- [21] Priest E R and Forbes T 2000 *Magnetic Reconnection* (Cambridge: Cambridge University Press)
- [22] Hughes D, Paczuski M, Dendy R O, Helander P and McClements K 2003 *Phys. Rev. Lett* **90** 131101
- [23] Schrijver C J *et al.* 1998 *Nature* **394** 152; see also <http://www.lmsal.com/carpet.htm>
- [24] Chapman S C 2000 *Phys. Rev. E*, **62** 1905
- [25] Dennis B R 1985 *Solar Phys.* **100** 465
- [26] Aschwanden M J *et al.* 2000 *Astrophys. J.* **535** 1047
- [27] Wheatland M J, Sturrock P A and McTiernan J M 1998 *Astrophys. J.* **509** 448
- [28] Charbonneau P, McIntosh S W, Liu H-L and Bogdan T J 2001 *Solar Phys.* **203** 321
- [29] Dendy R O and Chapman S C 2006 *Plasma Phys. Control. Fusion* **48** B313
- [30] Greenhough J, Chapman S C, Chaty S, Dendy R O and Rowlands G 2002 *Astron. Astrophys.* **385**, 693
- [31] Greenhough J, Chapman S C, Chaty S, Dendy R O and Rowlands G 2003 *Mon. Not. R. Astr. Soc.* **340**, 851
- [32] Greenhough J, Chapman S C, Dendy R O, Nakariakov V and Rowlands G, *Astron. Astrophys.* **409**, L17 (2003)
- [33] Dudson B D, Dendy R O, Kirk A, Meyer H and Counsell G C 2005 *Plasma Phys. Control. Fusion* **47** 885
- [34] Greenhough J, Chapman S C, Dendy R O and Ward D J 2003 *Plasma Phys. Control. Fusion* **45** 747
- [35] March T K, Chapman S C and Dendy R O 2005 *Physica D* **200** 171
- [36] March T K, Chapman S C and Dendy R O 2005 *Geophys. Res. Lett.* **32** L04101
- [37] Hnat B, Dudson B H, Dendy R O, Counsell G C and Kirk A R 2008 *Nucl. Fusion* **48** 085009
- [38] Dewhurst J M, Hnat B, Ohno N, Dendy R O, Masuzaki S, Morisaki T and Komori A 2008 *Plasma Phys. Control. Fusion* **50** 095013
- [39] Wicks R T, Chapman S C and Dendy R O 2007 *Phys. Rev. E* **75** 051125
- [40] Nicol R M, Chapman S C and Dendy R O 2008 *Astrophys. J.* **679** 862
- [41] Wicks R T, Chapman S C and Dendy R O 2009 *Astrophys. J* **690** 734
- [42] Ohno N, Masuzaki S, Miyoshi H, Takamura S, Budaev V P, Morisaki T, Ohyabu N and Komori A 2006 *Contrib. Plasma Phys.* **46** 692
- [43] Dendy R O, Helander P and Tagger M 1998 *Astron. Astrophys.* **337** 962
- [44] Benzi R, Ciliberto S, Trippicione R, Baudet C, Massaioli F and Succi S 1993 *Phys. Rev. E* **48** 29